42. Brown, A. J., and W. Jessup. 1999. Oxysterols and atherosclerosis. *Atherosclerosis.* **142:** 1–28.
43. Brown, M. S., S. E. Dana, and J. L. Goldstein. 1975. Cholesterol ester formation in cultured human fibroblasts. Stimulation by oxygenated sterols. *J. Biol. Chem.* **250:** 4025–4027.
44. Peng, S. K., P. Tham, C. B. Taylor, and B. Mikkelson. 1979. Cytotoxicity of oxidation derivatives of cholesterol on cultured aortic smooth muscle cells and their effect on cholesterol biosynthesis. *Am. J. Clin. Nutr.* **32:** 1033–1042.
45. Chang, T. Y., and J. S. Limanek. 1980. Regulation of cytosolic acetoacetyl coenzyme A thiolase, 3-hydroxy-3-methylglutaryl coenzyme A synthase, 3-hydroxy-3-methylglutaryl coenzyme A reductase, and mevalonate kinase by low density lipoprotein and by 25-hydroxycholesterol in Chinese hamster ovary cells. *J. Biol. Chem.* **255:** 7787–7795.
46. Yang, J., R. Sato, J. L. Goldstein, and M. S. Brown. 1994. Sterol-resistant transcription in CHO cells caused by gene rearrangement that truncates SREBP-2. *Genes Dev.* **8:** 1910–1919.
47. Yang, J., M. S. Brown, Y. K. Ho, and J. L. Goldstein. 1995. Three different rearrangements in a single intron truncate sterol regulatory element binding protein-2 and produce sterol-resistant phenotype in three cell lines. Role of introns in protein evolution. *J. Biol. Chem.* **270:** 12152–12161.
48. Hua, X., A. Nohturfft, J. L. Goldstein, and M. S. Brown. 1996. Sterol resistance in CHO cells traced to point mutation in SREBP cleavage-activating protein. *Cell.* **87:** 415–426.
49. Cadigan, K. M., J. G. Heider, and T. Y. Chang. 1988. Isolation and characterization of Chinese hamster ovary cell mutants deficient in acyl-coenzyme A:cholesterol acyltransferase activity. *J. Biol. Chem.* **263:** 274–282.
50. Metherall, J. E., N. D. Ridgway, P. A. Dawson, J. L. Goldstein, and M. S. Brown. 1991. A 25-hydroxycholesterol-resistant cell line deficient in acyl-CoA: cholesterol acyltransferase. *J. Biol. Chem.* **266:** 12734–12740.
51. Cheng, D., C. C. Chang, X. Qu, and T. Y. Chang. 1995. Activation of acyl-coenzyme A:cholesterol acyltransferase by cholesterol or by oxysterol in a cell-free system. *J. Biol. Chem.* **270:** 685–695.
52. Lichtenstein, A. H., and P. Brecher. 1983. Esterification of cholesterol and 25-hydroxycholesterol by rat liver microsomes. *Biochim. Biophys. Acta.* **751:** 340–348.
53. Shibata, N., A. F. Carlin, N. J. Spann, K. Saijo, C. S. Morello, J. G. McDonald, C. E. Romanoski, M. R. Maurya, M. U. Kaikkonen, M. T. Lam, et al. 2013. 25-Hydroxycholesterol activates the integrated stress response to reprogram transcription and translation in macrophages. *J. Biol. Chem.* **288:** 35812–35823.
54. Bansal, N., A. Houle, and G. Melnykovych. 1991. Apoptosis: mode of cell death induced in T cell leukemia lines by dexamethasone and other agents. *FASEB J.* **5:** 211–216.
55. Baldán, A., L. Pei, R. Lee, P. Tarr, R. K. Tangirala, M. M. Weinstein, J. Frank, A. C. Li, P. Tontonoz, and P. A. Edwards. 2006. Impaired development of atherosclerosis in hyperlipidemic Ldlr-/- and ApoE-/- mice transplanted with Abcg1-/- bone marrow. *Arterioscler. Thromb. Vasc. Biol.* **26:** 2301–2307.
56. Infante, R. E., A. Radhakrishnan, L. Abi-Mosleh, L. N. Kinch, M. L. Wang, N. V. Grishin, J. L. Goldstein, and M. S. Brown. 2008. Purified NPC1 protein: II. Localization of sterol binding to a 240-amino acid soluble luminal loop. *J. Biol. Chem.* **283:** 1064–1075.
57. Bauman, D. R., A. D. Bitmansour, J. G. McDonald, B. M. Thompson, G. Liang, and D. W. Russell. 2009. 25-Hydroxycholesterol secreted by macrophages in response to Toll-like receptor activation suppresses immunoglobulin A production. *Proc. Natl. Acad. Sci. USA.* **106:** 16764–16769.
58. Liu, S. Y., R. Aliyari, K. Chikere, G. Li, M. D. Marsden, J. K. Smith, O. Pernet, H. Guo, R. Nusbaum, J. A. Zack, et al. 2013. Interferon-inducible cholesterol-25-hydroxylase broadly inhibits viral entry by production of 25-hydroxycholesterol. *Immunity.* **38:** 92–105.
59. Blanc, M., W. Y. Hsieh, K. A. Robertson, K. A. Kropp, T. Forster, G. Shui, P. Lacaze, S. Watterson, S. J. Griffiths, N. J. Spann, et al. 2013. The transcription factor STAT-1 couples macrophage synthesis of 25-hydroxycholesterol to the interferon antiviral response. *Immunity.* **38:** 106–118.

Journal of Plastic, Reconstructive & Aesthetic Surgery (2014) 67, 205–211

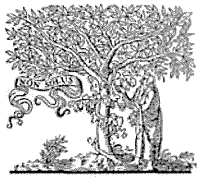

ELSEVIER

JPRAS
An International Journal of Surgical Reconstruction
www.JPRASurg.com

Postoperative patency of the retrograde internal mammary vein anastomosis in free flap transfer☆

Yoshitaka Kubota*, Nobuyuki Mitsukawa, Shinsuke Akita, Masakazu Hasegawa, Kaneshige Satoh

Department of Plastic Surgery, Chiba University, 1-8-1, Inohana, Chuo-ku, Chiba-city, Chiba 260-8677, Japan

Received 15 June 2013; accepted 7 October 2013

KEYWORDS
Internal mammary vein;
Free flap;
Retrograde

Summary *Background and aim:* A caudal limb of the internal mammary vein (IMV) can be used as an additional venous drainage route in free flap transfer. However, there remains the possibility that unrecognised occlusion of the retrograde IMV occurs in the early postoperative period due to non-physiologic flow, thus affecting venous drainage. There are no reports regarding the postoperative patency rates of the anastomosed retrograde IMV. This study aimed to clarify the efficacy of the retrograde IMV as an additional venous drainage route in the case of two-vein anastomosis in free flap transfer.
Patients and methods: We performed a hospital-based prospective case series study to clarify the patency rates of retrograde IMV anastomoses as an additional venous drainage route in cases of two-vein anastomosis in free flap transfer. Both antegrade and retrograde IMV anastomoses were performed in patients who underwent free flap transfer using the IMV as a recipient vein. The postoperative flow vector and peak blood velocity of the retrograde IMV anastomosis were examined using two-dimensional phase contrast magnetic resonance imaging (2D PC-MRI) and colour Doppler imaging.
Result: A total of five retrograde IMV anastomoses in five patients were performed in the study period. The postoperative patency rate of the retrograde IMV was 60%. In the patent group, the postoperative peak venous blood velocity of the retrograde IMV was significantly slower than that of the antegrade IMV (4.6 ± 0.5 vs 7.2 ± 0.8 cm s^{-1}, $P < 0.05$).

☆ Part of this work was presented at the 38th Annual Meeting of the Japan Society for Reconstructive Microsurgery, Niigata, Japan, 10–11 November 2011.

* Corresponding author. Tel./fax: +81 43 226 2316.
E-mail address: kubota-cbu@umin.ac.jp (Y. Kubota).

http://dx.doi.org/10.1016/j.bjps.2013.10.013

Conclusion: We described the postoperative patency rate of retrograde IMV anastomosis in cases of two-vein anastomosis in free flap transfer. Further study is needed to evaluate the reliability of the retrograde IMV as an additional venous drainage route.

Background

Use of a caudal limb of the internal mammary vein (IMV) as an additional venous drainage route was first reported by Kerr-Valentic et al., with subsequent reports from other authors.[1–4] Initially, the efficacy of the retrograde IMV anastomosis was based on the hypothesis that because the IMV has no valves, venous blood should flow from the flap vein into the retrograde IMV in accordance with pressure gradients insofar as venous pressure of the flap vein is higher than that of the retrograde IMV. However, this hypothesis was disproven by Mackey et al., who showed that 44% of cadavers had valves in at least one IMV.[5] Mohebali et al. reported that intra-operative flow into the retrograde IMV occurred a few seconds later than that into the antegrade IMV in a study using laser-assisted indocyanine green angiography.[3] Venturi et al. reported that intra-operative mean blood flow in the retrograde IMV was less than that in the antegrade IMV in a study using a Doppler ultrasound technique.[2] This evidence suggests that non-physiologic flow from the retrograde IMV may generate an increased pressure gradient that needs to be overcome. No reports are available regarding the postoperative flow of the anastomosed retrograde IMV. We prospectively investigated the postoperative patency of such anastomoses.

Objective

The objective of this study is to clarify the efficacy of the retrograde IMV as an additional venous drainage route in the case of two-vein anastomosis in free flap transfer.

Study design, setting

We performed a hospital-based prospective case series study. The study protocol was approved by the ethical committee of Chiba University. All patients provided written informed consent to participate in this study.

Patients and methods

Patient selection and study protocol

Patients who underwent free flap surgery at Chiba University Hospital from August 2011 to March 2012 using the IMV as a recipient vein with both of the following conditions were included in the study:

A) only one IMV suitable for microanastomosis and
B) more than one flap vein suitable for microanastomosis.

Patient data regarding age, sex, body weight, height, medical co-morbidities, type of surgery, radiation, type of flap, number of perforators, donor vein, coupler size, postoperative course and postoperative patency and peak blood velocity of the retrograde IMV were collected prospectively.

Surgical procedure

Under general anaesthesia, internal mammary vessels were exposed via resection of one or two rib cartilages. The deep inferior epigastric artery (DIEA) was anastomosed to the internal mammary artery (IMA) in an end-to-end fashion. The IMV was cut at the mid-point of the exposed area. One of the free flap veins which had the largest calibre was anastomosed to the cephalad end of the IMV (antegrade IMV) in an end-to-end fashion using a coupler. One of the free flap veins, which had the second largest calibre, was anastomosed to the caudal end of the IMV (retrograde IMV) in an end-to-end fashion using a coupler. Intra-operative venous flow into the retrograde IMV was observed by microscope-integrated near-infrared indocyanine green angiography.[3,6]

Blood flow analysis

Analyses determining the patency and direction of flow were performed 6 months after the operation. Peak venous blood velocity was measured using colour Doppler imaging in all patients using the EUB-7500 ultrasound system (Hitachi Medical Corporation, Tokyo, Japan) with a 4–16-MHz linear probe held at an angle of 45° to the vein.[7]

Antegrade IMV

The flow vector of the antegrade IMV was determined by Doppler spectrum using the accompanying artery as a reference.[8]

Retrograde IMV

The flow vector of the retrograde IMV was determined by one or two imaging modalities, namely colour Doppler imaging and two-dimensional phase contrast magnetic resonance imaging (2D PC-MRI).[9–13] This technique was used if the superficial inferior epigastric vein (SIEV) was anastomosed to the retrograde IMV. It was not adopted if two deep inferior epigastric veins (DIEVs) were used for anastomosis because their close proximity decreases the technique's validity.

Table 1 Characteristics of the patients who underwent the retrograde internal mammary vein anastomosis in free flap transfer.

Patient	Sex	Age	BMI[a]	Co-morbidity	Purpose of surgery	Radiation	Type of flap	Number of perforators
1	Female	65	19	None	Reconstruction of chest radiation ulcer	Yes	VRAM[b]	3
2	Female	49	21	Cigarette smoker	Breast reconstruction	No	DIEP[c]	1
3	Female	63	19	Diabetes mellitus	Breast reconstruction	No	DIEP	1
4	Female	57	25	None	Breast reconstruction	No	MS-TRAM[d]	2
5	Female	45	28	Cigarette smoker, hyperlipidaemia	Breast reconstruction	No	DIEP	1

[a] BMI denotes body mass index. BMI was calculated as follows: Body weight (kg)/Height (m)/Height (m).
[b] VRAM denotes vertical rectus abdominis muscle.
[c] DIEP denotes deep inferior epigastric perforator.
[d] MS-TRAM denotes muscle sparing transverse rectus abdominis muscle.

Statistical analysis

Continuous variables were compared with the Student's *t*-test under the condition that equal variances could be assumed by Levene's test. Welch's *t*-test was used if equal variances could not be assumed by Levene's test. All *P* values quoted are two tailed. *P* values <0.05 were considered to indicate statistical significance. Statistical analyses were conducted using SPSS software (version 13.0J; SPSS, Chicago, IL, USA).

Result

A total of five patients met the criteria for the study in the study period (Table 1). Five retrograde IMV anastomoses were performed in five flaps in five patients (Tables 1 and 2). Intra-operative venous flow into the retrograde IMV was confirmed by microscope-integrated near-infrared indocyanine green angiography in all patients[3,6]; all flaps survived. Postoperative measurement of the blood flow of the IMV was performed easily with the EUB-7500 ultrasound system in all patients.

Postoperative flow

Antegrade IMV

The flow vector from the DIEV to the antegrade IMV was confirmed by Doppler spectrum using the accompanying artery as a reference in all patients (Figures 1A and 2).[8]

Retrograde IMV

In three of five patients, postoperative patency of the retrograde IMV anastomosis was confirmed (patent group, patients 1, 2 and 3), whereas postoperative occlusion of the retrograde IMV anastomosis was confirmed in two patients (occluded group, patients 4 and 5) (Table 2).

In the patent group, the postoperative course was uneventful and the flow vector from the flap vein to the retrograde IMV was confirmed by colour Doppler imaging in all patients (Figures 1B and 2). The peak venous blood velocity of the retrograde IMV was significantly slower than that of the antegrade IMV (4.6 ± 0.5 vs 7.2 ± 0.8 cm s^{-1} (mean $\pm$ standard deviation (SD)), $P < 0.05$). In patient 1, 2D PC-MRI showed that blood flowed in the direction from the SIEV to the retrograde IMV (Figure 1B); 2D PC-MRI also showed dilation of the SIEV.

Table 2 Postoperative flow of the retrograde internal mammary vein anastomoses.

Patient	Flap vein and coupler size (mm)				Postoperative patency of retrograde IMV[a] and confirmation procedure		Postoperative peak venous blood velocity (cm/s)		Postoperative course
	Antegrade IMV		Retrograde IMV				Antegrade IMV	Retrograde IMV	
1	DIEV[b]	2.0	SIEV[c]	2.0	Patent	US[d] and 2D PC-MRI[e]	6.5	4.2	Uneventful
2	DIEV1	2.0	DIEV2	2.0	Patent	US	7.0	5.1	Uneventful
3	DIEV1	2.0	DIEV2	2.0	Patent	US	8.1	4.6	Uneventful
4	DIEV1	2.5	DIEV2	2.5	Occluded	Exploration	11.7	–	Slight congestion
5	DIEV1	3.0	DIEV2	2.0	Occluded	US	15.2	–	Uneventful

[a] IMV denotes internal mammary vein.
[b] DIEV denotes deep inferior epigastric vein.
[c] SIEV denotes superficial inferior epigastric vein.
[d] US denotes ultrasound.
[e] 2D-PC MRI denotes two dimensional phase contrast magnetic resonance imaging.

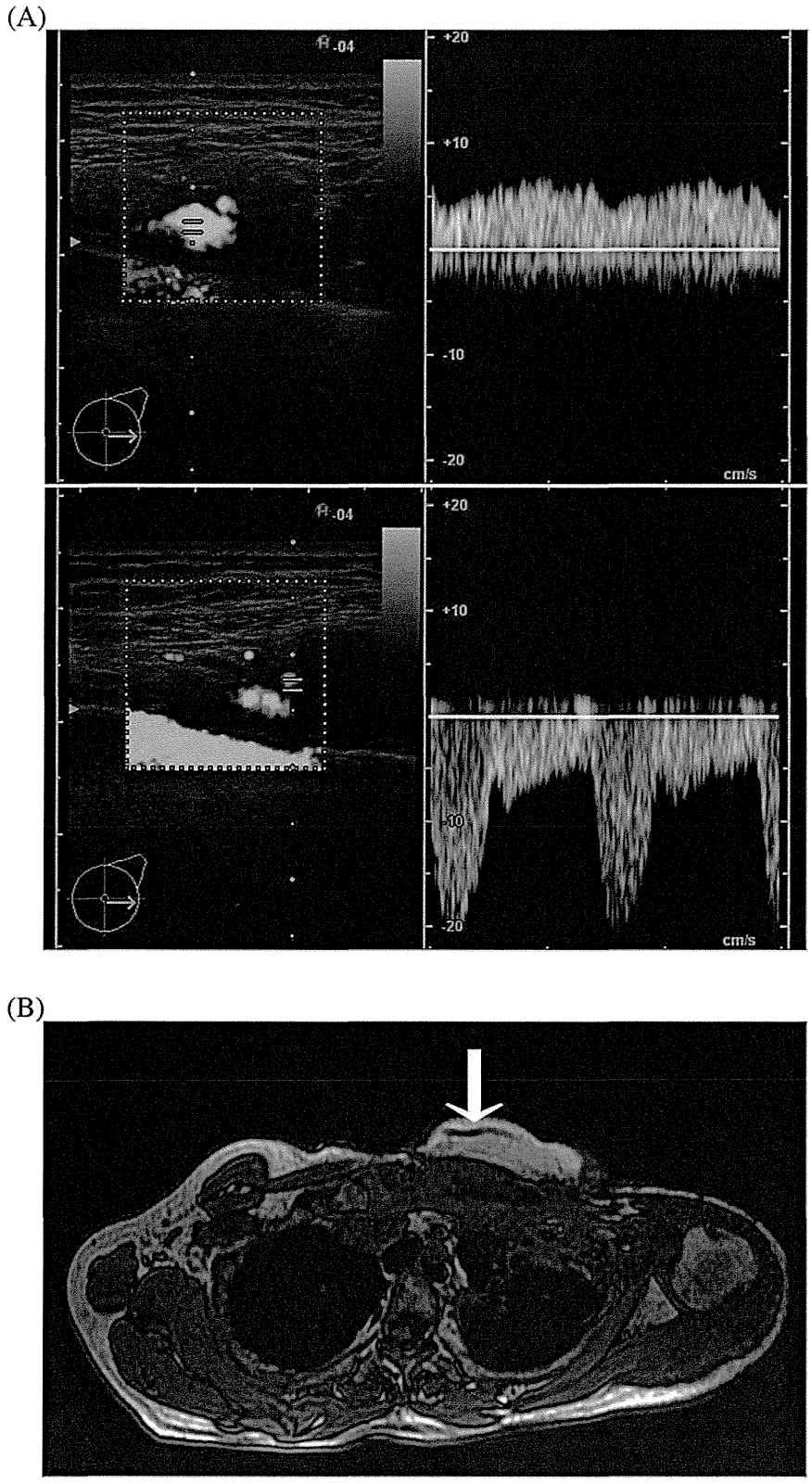

Figure 1 (A) Doppler spectrum of the DIEV (*above*) anastomosed to the antegrade IMV and the DIEA (*below*) six months postoperatively in patient 1. Doppler spectrum of the DIEV was opposite to that of the accompanying DIEA. This indicates that the flow direction is from the DIEV to the antegrade IMV. (B) Phase contrast two-dimensional magnetic resonance imaging six months postoperatively in patient 1. An arrow indicates a dilated SIEV anastomosed to the retrograde IMV running in the subcutaneous tissue of the flap. Parameter (not shown) indicates the direction of flow is from the SIEV to the retrograde IMV.

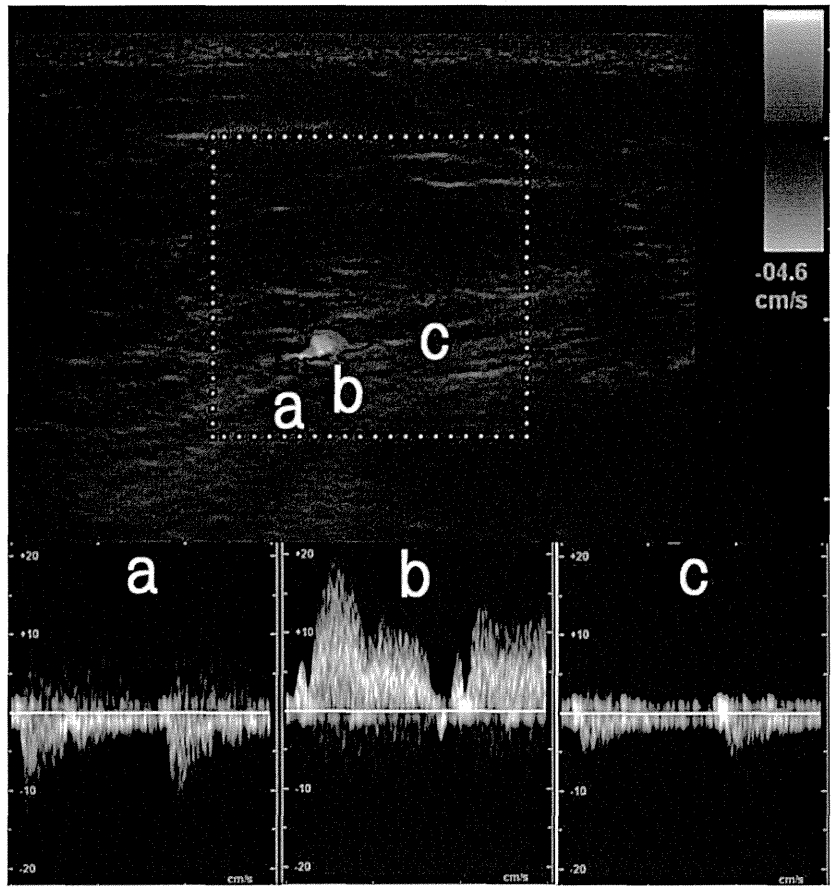

Figure 2 Doppler spectrum of the DIEA (b) and DIEVs (a and c) in patient 2 six months postoperatively. DIEV1 (a) was anastomosed to the antegrade IMV and DIEV2 (c) was anastomosed to the retrograde IMV. The wave pattern shows that the direction of flow of the DIEVs (a and c) and DIEA (b) are opposite. The flow velocity of the DIEV2 (c) anastomosed to the retrograde IMV is lower than that of the DIEV1 (a) anastomosed to the antegrade IMV.

In one patient in the occluded group, the postoperative course was uneventful and there were no signs of venous congestion. However, occlusion of the retrograde IMV was confirmed by colour Doppler imaging 6 months postoperatively (patient 5). In the other patient in this group, occlusion of the retrograde IMV was confirmed during re-exploration of the anastomosis site, which was performed 18 h after the original operation for slight congestion of the flap (patient 4). It was unclear whether valves were present in the retrograde IMV in this case. We did not perform an additional venous anastomosis. The slight congestion of the flap lessened over time in the postoperative period.

Discussion

The underlying hypothesis for performing a retrograde IMV anastomosis is that because the pressure of the retrograde IMV is lower than that of the flap vein, and because the IMV lacks valves, venous blood from the flap can flow into the retrograde IMV according to a pressure gradient.[1] However, an increased pressure gradient due to non-physiologic flow from the retrograde IMV was suggested by Mohebali et al. and Venturi et al.[2,3] Our measurements showing that the peak venous blood velocity of the flap vein anastomosed to the retrograde IMV was slower than that of the flap vein anastomosed to the antegrade IMV suggest that there is high resistance of the retrograde IMV as a venous drainage route. In our study, dilation of the SIEV anastomosed to the retrograde IMV also suggests a high gradient into the retrograde IMV.

A limited number of reports are available describing venous pressure values of the IMV and the pedicle vein of the free flap.[14–16] Our study shows that at least in some patients, the venous pressure of the flap vein remains higher than that of the retrograde IMV under the condition that the antegrade IMV is patent. According to one report of accidental insertion of a central venous catheter into the IMV, the intravascular pressure of the IMV was 5 mmHg.[14] Sakurai et al. reported that the venous pressure of the vein of a transferred free flap measured by catheter was anywhere from 0 to 35 mmHg.[15] Smit et al. reported that the venous pressure of the SIEV which is ipsilateral to the pedicle of the deep inferior epigastric perforator (DIEP) flap ranged from 0 to 24 mmHg.[16]

It was difficult to infer the presence or absence of valves in the retrograde IMV in our study. Mackey et al. reported that 14 of 32 cadavers had valves in the IMV,

whereas Al-Dhamin et al. reported that there were no valves in five cadavers.[4,5] Timmons hypothesised that three conditions occurring simultaneously were necessary for reverse flow through a valve: denervation, higher proximal venous pressure than distal and constant blood supply.[17] Torii et al. reported that reflux of venous blood through a valve occurred at pressures of 66–77 mmHg.[18] These conditions suggest that reverse flow through a valve in the retrograde IMV is difficult when venous blood can flow into the antegrade IMV.[14] Collateral vessels play a critical role in venous drainage through the retrograde IMV.[4,5,19,20] An increased pressure gradient caused by a valve or by insufficient collateral vessels can lead to decreased patency rate of the retrograde IMV anastomosis, as found in our study. Further investigation is needed to determine the postoperative patency rate of the retrograde IMV and its relationship to the valves and collateral pathways of the IMV.

Based on our findings, retrograde IMV anastomosis is not reliable enough to be routinely performed. We prefer performing an anastomosis of only the antegrade IMV rather than performing anastomoses of both the antegrade and retrograde IMVs even in the case of two DIEVs and only one IMV. One of the drawbacks of using the retrograde IMV is a short working length of the antegrade and the retrograde IMVs as they are cut at the mid-point of the exposed IMV. Using only an antegrade IMV by cutting the caudal edge of the exposed IMV can ensure adequate working length for an easy anastomosis.[21–27] Hanasono et al. argued against routinely performing two venous anastomoses, explaining that venous blood velocity in flaps in which two venous anastomoses were performed was significantly slower than that in flaps in which one venous anastomosis was performed.[7] Measurements in our study showed that peak venous blood velocity of the antegrade IMV in the patent group in which both the antegrade and retrograde IMVs functioned was lower than that in the occluded group in which only the antegrade IMV functioned; these results are consistent with the report by Hanasono et al.[7] In the cases in which double venous systems (namely, an SIEV system and a DIEV system) are required, the use of other antegrade veins is reported as an additional venous drainage route rather than a retrograde IMV.[28–31]

Conclusion

The postoperative flow vector and peak venous blood velocity of retrograde IMV anastomosis in two-vein anastomosis cases were studied for the first time, to our knowledge. Our study showed a 60% patency rate of the retrograde IMV anastomosis under two-vein anastomosis operations. The peak venous blood velocity of the free flap vein anastomosed to the retrograde IMV was significantly slower than that of the free flap vein anastomosed to the antegrade IMV. Further study is needed to evaluate the efficacy of the retrograde IMV as an additional venous drainage route.

Funding

None.

Conflicts of interest

None declared.

References

1. Kerr-Valentic MA, Gottlieb LJ, Agarwal JP. The retrograde limb of the internal mammary vein: an additional outflow option in DIEP flap breast reconstruction. *Plast Reconstr Surg* 2009;**124**: 717–21.
2. Venturi ML, Poh MM, Chevray PM, Hanasono MM. Comparison of flow rates in the antegrade and retrograde internal mammary vein for free flap breast reconstruction. *Microsurgery* 2011;**31**: 596–602.
3. Mohebali J, Gottlieb LJ, Agarwal JP. Further validation for use of the retrograde limb of the internal mammary vein in deep inferior epigastric perforator flap breast reconstruction using laser-assisted indocyanine green angiography. *J Reconstr Microsurg* 2010;**26**:131–5.
4. Al-Dhamin A, Bissell MB, Prasad V, Morris SF. The use of retrograde limb of internal mammary vein in autologous breast reconstruction with DIEAP flap: anatomical and clinical study. *Ann Plast Surg* 2013 [Epub ahead of print].
5. Mackey SP, Ramsey KW. Exploring the myth of the valveless internal mammary vein – a cadaveric study. *J Plast Reconstr Aesthet Surg* 2011:1174–9.
6. Holm C, Mayr M, Höfter E, Dornseifer U, Ninkovic M. Assessment of the patency of microvascular anastomoses using microscope-integrated near-infrared angiography: a preliminary study. *Microsurgery* 2009;**29**:509–14.
7. Hanasono MM, Kocak E, Ogunleye O, Hartley CJ, Miller MJ. One versus two venous anastomoses in microvascular free flap surgery. *Plast Reconstr Surg* 2010;**126**:1548–57.
8. Kuzo RS, Ben-Ami TE, Yousefzadeh DK, Ramirez JG. Internal mammary compartment: window to the mediastinum. *Radiology* 1995;**195**:187–92.
9. Alonso-Burgos A, Garcia-Tutor E, Bastarrika G, Benito A, Dominguez PD, Zubieta JL. Preoperative planning of DIEP and SGAP flaps: preliminary experience with magnetic resonance angiography using 3-tesla equipment and blood-pool contrast medium. *J Plast Reconstr Aesthet Surg* 2010;**63**:298–304.
10. Kudo K, Terae S, Ishii A, et al. Physiologic change in flow velocity and direction of dural venous sinuses with respiration: MR venography and flow analysis. *Am J Neuroradiol* 2004;**25**: 551–7.
11. Neil-Dwyer JG, Ludman CN, Schaverien M, McCulley SJ, Perks AG. Magnetic resonance angiography in preoperative planning of deep inferior epigastric artery perforator flaps. *J Plast Reconstr Aesthet Surg* 2009;**62**:1661–5.
12. Rubino C, Ramakrishnan V, Figus A, Bulla A, Coscia V, Cavazzuti MA. Flap size/flow rate relationship in perforator flaps and its importance in DIEAP flap drainage. *J Plast Reconstr Aesthet Surg* 2009;**62**:1666–70.
13. Han S, Yoon SY, Park JM. The anatomical evaluation of internal mammary vessels using sonography and 2-dimensional computed tomography in Asians. *Br J Plast Surg* 2003;**56**: 684–8.
14. Sandroni C, Pirronti T, Tortora F, Santangelo S, Rinaldi P, Antonelli M. Unusual central venous catheter malposition into the left internal mammary vein: a case report. *Intensive Care Med* 2003;**29**:2338–9.
15. Sakurai H, Nozaki M, Takeuchi M, et al. Monitoring the changes in intraparenchymatous venous pressure to ascertain flap viability. *Plast Reconstr Surg* 2007;**119**:2111–7.
16. Smit JM, Audolfsson T, Whitaker IS, Werker PM, Acosta R, Liss AG. Measuring the pressure in the superficial inferior

epigastric vein to monitor for venous congestion in deep inferior epigastric artery perforator breast reconstructions: a pilot study. *J Reconstr Microsurg* 2010;**26**:103–7.
17. Timmons MJ. The vascular basis of the radial forearm flap. *Plast Reconstr Surg* 1986;**77**:80–92.
18. Torii S, Namiki Y, Mori R. Reverse-flow island flap: clinical report and venous drainage. *Plast Reconstr Surg* 1987;**79**: 600–9.
19. Clark CPI, Rohrich RJ, Copit S, Pittman CE, Robinson J. An anatomic study of the internal mammary veins: clinical implications for free-tissue-transfer breast reconstruction. *Plast Reconstr Surg* 1997;**99**:400–4.
20. Shigehara T, Tsukagoshi T, Satoh K, Tatezaki S, Ishii T. A reversed-flow latissimus dorsi musculocutaneous flap based on the serratus branch in primary shoulder reconstruction. *Plast Reconstr Surg* 1997;**99**:566–9.
21. Roche NA, Houtmeyers P, Vermeersch HF, Stillaert FB, Blondeel PN. The role of the internal mammary vessels as recipient vessels in secondary and tertiary head and neck reconstruction. *J Plast Reconstr Aesthet Surg* 2012;**65**:885–92.
22. Tuinder S, Dikmans R, Schipper RJ, et al. Anatomical evaluation of the internal mammary vessels based on magnetic resonance imaging (MRI). *J Plast Reconstr Aesthet Surg* 2012; **65**:1363–7.
23. Majumder S, Batchelor AG. Internal mammary vessels as recipients for free TRAM breast reconstruction: aesthetic and functional considerations. *Br J Plast Surg* 1999;**52**:286–9.
24. Ninkovic M, Anderl H, Hefel L, Schwabegger A, Wechselberger G. Internal mammary vessels: a reliable recipient system for free flaps in breast reconstruction. *Br J Plast Surg* 1995;**48**:533–9.
25. Hefel L, Schwabegger A, Ninkovic M, et al. Internal mammary vessels: anatomical and clinical considerations. *Br J Plast Surg* 1995;**48**:527–32.
26. Figus A, Mosahebi A, Ramakrishnan V. Microcirculation in DIEP flaps: a study of the haemodynamics using laser Doppler flowmetry and lightguide reflectance spectrophotometry. *J Plast Reconstr Aesthet Surg* 2006;**59**:604–12 [discussion 13].
27. Yagi S, Kamei Y, Fujimoto Y, Torii S. Use of the internal mammary vessels as recipient vessels for an omental flap in head and neck reconstruction. *Ann Plast Surg* 2007;**58**:531–5.
28. Boutros SG. Double venous system drainage in deep inferior epigastric perforator flap breast reconstruction: a single-surgeon experience. *Plast Reconstr Surg* 2013;**131**:671–6.
29. Enajat M, Rozen WM, Whitaker IS, Smit JM, Acosta R. A single center comparison of one versus two venous anastomoses in 564 consecutive DIEP flaps: investigating the effect on venous congestion and flap survival. *Microsurgery* 2010;**30**:185–91.
30. Guzzetti T, Thione A. The basilic vein: an alternative drainage of DIEP flap in severe venous congestion. *Microsurgery* 2008; **28**:555–8.
31. Ali R, Bernier C, Lin YT, et al. Surgical strategies to salvage the venous compromised deep inferior epigastric perforator flap. *Ann Plast Surg* 2010;**65**:398–406.

CLINICAL REPORT

AMERICAN JOURNAL OF medical genetics PART A

Low-Level Mesodermal Somatic Mutation Mosaicism: Late-Onset Craniofacial and Cervical Spinal Hyperostoses

Yoshitaka Kubota*, Nobuyuki Mitsukawa, Michiko Uchida, Yuuki Uchida, Shinsuke Akita, Masakazu Hasegawa and Kaneshige Satoh

Department of Plastic Surgery, Chiba University, Chiba-city, Chiba, Japan

Manuscript Received: 3 June 2013; Manuscript Revised: 24 September 2013; Manuscript Accepted: 3 October 2013

Craniofacial and cervical spinal hyperostoses are rarely seen in the absence of other abnormalities. Only seven patients with isolated cranial hyperostoses have been reported, and only a single patient with both calvarial and cervical vertebral hyperostoses. We report on an adult with late-onset right-sided asymmetrical hyperostoses of the cranium, mandible, and cervical vertebrae in the absence of an *AKT1* mutation. At presentation, the patient displayed neither generalized overgrowth nor dysregulated adipose tissue. Standard polymerase chain reaction and Sanger sequencing of DNA extracted from formalin-fixed paraffin-embedded frontal bone and mandibular angular bone was negative for an *AKT1* mutation. Though the patient's clinical manifestations did not fulfill the consensus diagnostic criteria of Proteus syndrome, the mosaic distribution of lesions, the sporadic occurrence, and the patient's progressive course were consistent with a somatic mosaicism similar to that syndrome. Hence, the patient's phenotype may have been caused by a very late mesodermal somatic mutation during embryogenesis.

Key words: hyperostosis; Proteus syndrome; v-akt murine thymoma viral oncogene homolog 1

How to Cite this Article:
Kubota Y, Mitsukawa N, Uchida M, Yuuki U, Akita S, Hasegawa M, Satoh K. 2013. Low-level mesodermal somatic mutation mosaicism: Late-onset craniofacial and cervical spinal hyperostoses.
Am J Med Genet Part A 9999:1–7.

INTRODUCTION

Craniofacial and cervical spinal hyperostoses with neither generalized overgrowth nor other abnormalities are rare clinical entities. A literature search reveals only seven reported patients with cranial hyperostoses who did not have associated anomalies [Pagon et al., 1986; Smeets et al., 1994; Nishimura and Nishimura, 1997; Adolphs et al., 2011; Kannu et al., 2011]. Of these, only one patient had both calvarial and cervical vertebral hyperostoses [Kannu et al., 2011]. We report herein on a 20-year-old Asian male with right-sided asymmetrical craniofacial and cervical spinal hyperostosis that was first noted after puberty.

CLINICAL REPORT

The patient, an Asian male, was born at 38 weeks after a normal gestation to a healthy 23-year-old mother and a non-consanguineous healthy 23-year-old father. His birth weight was 2,698 g (10th–25th centile). His head circumference at birth was 31.5 cm (3rd–10th centile). He displayed no physical anomalies at birth and followed a normal growth and development pattern, with no sign of intellectual disability or learning disability. No family member had a genetic disorder, craniofacial hyperostoses, polyps of the gastrointestinal tract, vascular or lymphatic malformations, soft-tissue hypertrophy, neurofibromatosis, megalencephaly, or dysregulation of adipose tissue (such as multiple lipomas or localized absence of adipose tissue). He had one healthy younger brother.

At age 20 years the patient presented to our clinic with a 6-year history of multiple painless lumps at the right mandibular angle, the right paramedian forehead, the hair-bearing right frontoparietal region, the right occipitoparietal region, and the right mastoid (Fig. 1). He first noticed the lumps in the right frontoparietal area and the right mastoid area at age 14 years, followed by lesions on the right paramedian forehead at 16 years and the right mandibular angle at 18 years. Each lump continued to enlarge slowly. His medical history was otherwise unremarkable. He worked in a factory, but had no history of exposure to environmental carcinogens.

Conflict of Interest: The authors declare that no conflicts of interest exist.

*Correspondence to:
Yoshitaka Kubota, M.D., Department of Plastic Surgery, Chiba University, 1-8-1, Inohana, Chuo-ku, Chiba-city, Chiba #260-8677, Japan. E-mail: kubota-cbu@umin.ac.jp

Article first published online in Wiley Online Library (wileyonlinelibrary.com): 00 Month 2013
DOI 10.1002/ajmg.a.36310

FIG. 1. Preoperative photographs showing normal facial phenotype and bony protuberances of the right paramedian frontal area, the right mandibular area, and the right retroauricular area (arrow, B).

He had no smoking history and denied headache, dizziness, nausea, or palsy. He did complain of auditory disturbances and tinnitus in the right ear.

On physical examination, he was 173 cm tall and weighed 57 kg. His growth and development appeared normal, and his facial appearance was normal (Fig. 1A). He displayed no oculomotor disturbances, strabismus, or other neurologic deficits. The tumors had the hard consistency of bone. While the tumors themselves were immobile on the skull and the mandible, the scalp and the overlying facial skin moved freely over them. Dental examination showed a mouth-opening limitation of 25 mm and crepitation of the bilateral temporomandibular joints without deflection or pain. His teeth appeared normal and the remainder of the oral examination was normal.

The shape of his chest was normal. His abdomen was soft and flat, without tenderness or masses. No cerebriform connective-tissue nevi or epidermal nevi were observed. He had no apparent vascular malformation, lymphatic malformation, or subcutaneous tumor suggestive of epidermoid cysts or lipomatous tumors. The shape and skin of his external genitalia were normal. The length, circumference, and shape of his extremities were within normal ranges, and there was no significant asymmetry. His muscle strength and the range of motion of his extremities were normal. The range of motion of his neck was almost normal. There were no signs suggesting cervical radiculopathy or myelopathy on orthopedic examination.

Cephalography showed uniform-density bony thickening without periosteal reaction in the frontal, frontoparietal, occipital, right mastoid, and right mandibular areas. Rotational panoramic dental radiography showed hypertrophy of the right mandibular body, angle, and ramus without dental dysmorphology (Fig. 2). There were no odontomas or impacted teeth.

Computed tomography (CT) of the head showed normal brain structure and density. The cerebral hemispheres were symmetric, the structure of the gyri and sulci and the density of the cortex and subcortex were maintained, and there was no midline shift or enlargement of the ventricles. Hyperostoses were present at the right paramedian area of the frontal bone, from the mid to right side of the frontoparietal bones along the coronal suture, at the right occipitoparietal area along the right lambdoid suture, at the mastoid area of the right temporal bone, in the right occipitomastoidal suture area, in the bilateral nuchal line area, and at the external occipital protuberance (Fig. 3A–C). The right mastoid cells were enlarged, although their pneumatization was preserved (Fig. 3D). The bony part of the right external auditory canal was stenosed by hyperostosis (Fig. 3D). On coronal CT, deformation of the right temporomandibular joint was observed to result from hyperostosis of the right temporal-bone mandibular fossa. The right mandibular head showed flattening. Hyperostosis of the right side of the mandible was most evident at the jaw angle. No hypertrophy or atrophy of associated soft tissues was evident, including the subcutaneous tissue, muscles, parotid gland, tongue, and parapharyngeal structures.

Neck CT revealed right-sided hyperostosis of the cervical spine from C1 to C5. This hyperostosis affected the right side of the cervical bodies, transverse processes, laminae, and spinous processes. Cervical hyperostoses bulged into the spinal canal and compressed the spinal cord at the C3 level, although no sign of radiculopathy or myelopathy was evident on neurological examination (Fig. 3E). The cervical deformities were most obvious in C2 and C3, and the right facet joint between C2 and C3 was almost